arXiv:1405.4150v1 [astro-ph.HE] 16 May 2014

Relativistic Disc lines

A.C. Fabian[1], E. Kara[1], M.L. Parker[1]
[1] Institute of Astronomy, University of Cambridge, Madingley Road, Cambridge CB3 0HA, UK
Email: acf@ast.cam.ac.uk

Abstract

Broad emission lines, particularly broad iron-K lines, are now commonly seen in the X-ray spectra of luminous AGN and Galactic black hole binaries. Sensitive NuSTAR spectra over the energy range of 3–78 keV and high frequency reverberation spectra now confirm that these are relativistic disc lines produced by coronal irradiation of the innermost accretion flow around rapidly spinning black holes. General relativistic effects are essential in explaining the observations. Recent results are briefly reviewed here.

Key words: black hole physics: accretion discs, X-rays: galaxies

1. Introduction

The innermost regions around a luminous accreting black hole consist of an accretion disc of ionized gas extending down to the Innermost Stable Circular Orbit (ISCO) allowed by General Relativity. Material within that radius plunges into the black hole. Differential rotation within the disc amplifies magnetic fields creating and powering a compact corona above and below the centre of the disc. Hot electrons in the corona inverse Compton scatter soft disc photons into a hard X-ray power-law continuum which carries most of the radiated primary luminosity in the X-ray band of Active Galactic Nuclei (AGN) and Hard State Galactic Black Hole Binaries (BHB).

Secondary emission is produced by irradiation of the accretion disc by the primary continuum. The resulting back-scattered, fluorescent and secondary thermal emission (Fig. 1) is known as the *reflection spectrum* (even though it does not obey the standard laws of reflection). Emission lines observed from the innermost parts of the disc where matter is travelling up to half the speed of light are relativistically broadened and skewed to the red (i.e. lower energies) by Doppler and gravitational shifts and are shaped by relativistic beaming – they are relativistic disc lines. Such lines were predicted 25 years ago (Fabian et al 1989) and first clearly seen with ASCA 5 years later (Tanaka et al 1995).

The reflection continuum is characterized by a broad hump above 10 keV, shaped at high energies by the Compton effect (photons lose energy when backscattered) and at low energies by photoelectric absorption. The line component is due to fluorescence, excitation and ionization of the reflecting gas. Computation of the total reflection spectrum is a non-linear process where the ionization state depends on the flux of irradiating photons (see Ross & Fabian 1993, 1995; Garcia et al 2014). The relativistic reflection spectrum is obtained by relativistically blurring the whole spectrum (Fig. 2). Its shape consists of a soft excess, a broad iron line and a Compton hump, all of which features are now regularly observed (Fig. 3).

Confirmation of this picture has emerged from discovery of the expected X-ray reverberation signatures, first clearly detected from iron-L emission (Fabian et al 2009) and then from iron-K (Zoghbi et al 2012). Following intrinsic luminosity variations of the corona, energy bands dominated by reflected emission lag behind bands dominated by the primary continuum. This is a simple consequence of the longer path taken by the reflected signal in reaching us.

2. NuSTAR Observations of Relativistic Lines

Iron is the most abundant element with a high fluorescent yield, so the iron-K emission line is a prominent feature of a typical reflection spectrum. Relativistic iron lines are common in AGN and in hard and intermediate state BHB and have been observed with many different satellites and detectors. Many observations show broad iron lines (see e.g. Miller 2007 and Fabian 2013 for reviews) and under the assumption that the inner radius inferred from the width of the line corresponds to the ISCO, black hole spin has been measured (See Brenneman in these Proceedings and Reynolds 2013).

Recently, NuSTAR has begun delivering high quality spectra from 3–78 keV covering the iron line and Compton hump. The spectrum of NGC1365, for example, is well fitted by a relativistic reflection model (Risaliti et al 2013). Many other AGN now also show the characteristic skewed iron line and Compton hump of reflection (Fig. 4). Many of these objects are consistent with rapidly spinning black holes, which leads to maximum blurrring. One AGN which has a milder spin is SWIFTJ2127 shown in Fig. 3 from Marinucci et al

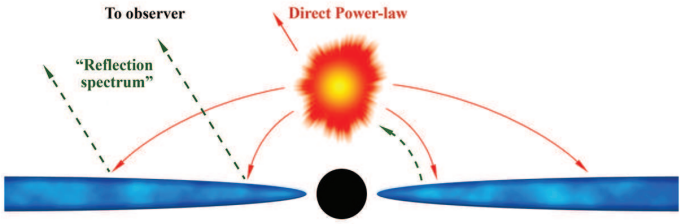

Fig. 1. Cartoon respresentation of the accretion disc and black hole with the corona above. The strong gravity causes causes primary emission from the corona to be bent down onto the disc. Backscattered and fluorescent and other secondary emission caused by irradiation of the disc forms the reflection spectrum.

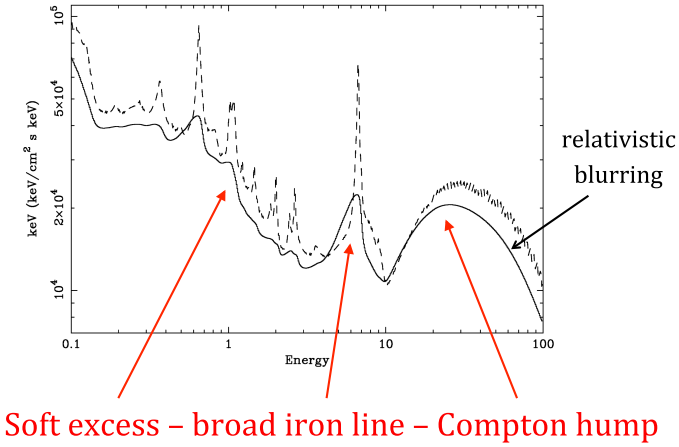

Fig. 2. The intrinsic reflection spectrum (dashed) is observed to be relativistically blurred (continuous line) by GR effects (from Ross & Fabian 2005).

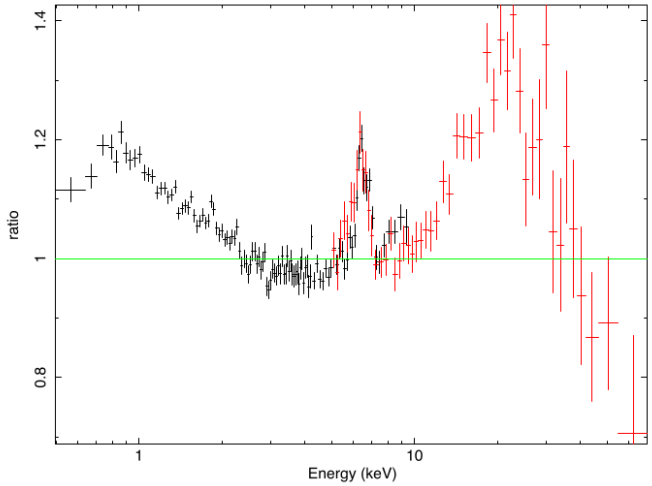

Fig. 3. XMM-NuSTAR spectrum of SWIFT J2127 (Marinucci et al 2013) shown as a ratio to a power-law. Note that all aspects of the reflection spectrum; the soft excess, the broad iron line and the Compton hump are seen here.

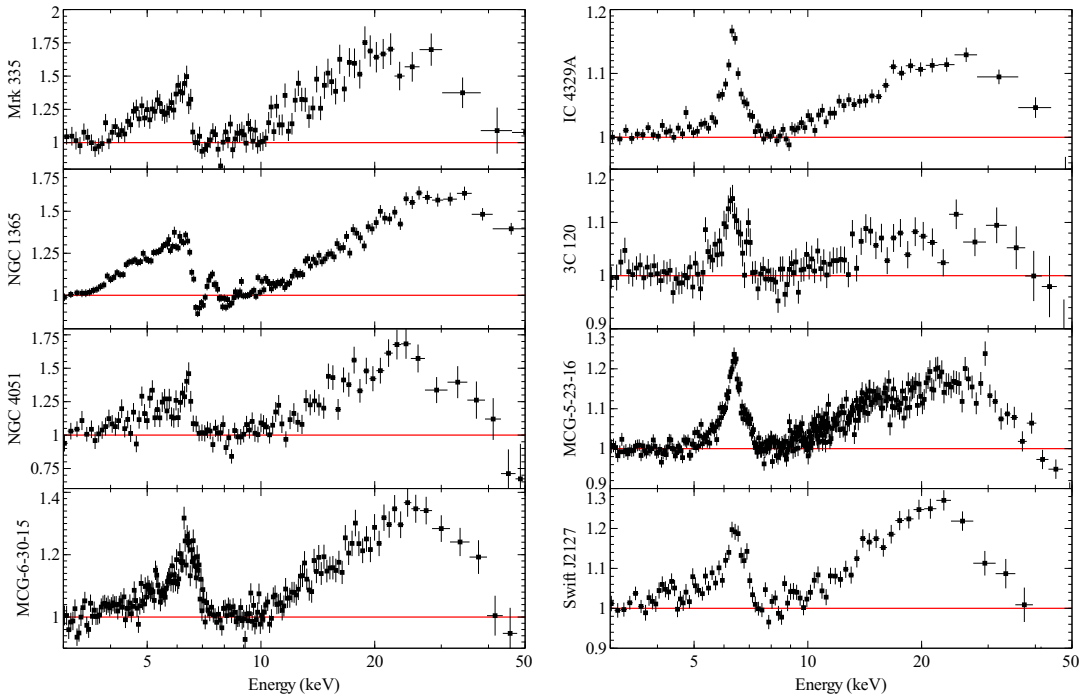

Fig. 4. NuSTAR spectra of a selection of AGN, shown as a ratio to a simple powerlaw fitted at 3-4 and 8-9 keV. Clockwise from top left are Mkn335, IC4329A, 3C120, MCG-5-23-16, SWIFTJ2127+5454, MCG–6-30-15, NGC4051 and NGC1365.

(2014). With the first imaging hard X-ray telescope for cosmic X-ray astronomy, NuSTAR gives excellent spectra of the Compton hump to several tens keV which enables detailed modelling to be carried out and the photon index of the primary continuum to be measured with accuracy.

Broad iron lines have been confirmed with NuSTAR in several BHB (GRO 1915, Miller et al 2013; Cyg X-1, Tomsick et al 2013) and even neutron stars (Ser X-1 Miller et al 2013). No distortion due to pile up is present in NuSTAR spectra even in bright sources like these.

One point to note here is that a very broad line implies not only that the black hole is spinning rapidly but also that at least part of the corona is close to the black hole at a height less than $\sim 10GM/c^2$ (Fabian et al 2014). If the corona is much further away then it does not illuminate the innermost regions sufficiently for the broad red wing to be clearly observed (see Fig. 5). Even if it is closer, then if the matter in the corona is flowing outward at a mild relativistic velocity, say at the base of a jet, then beaming can reduce the illumination of the disc and thus the broad red wing.

The corona does appear to be close to the black hole in many objects, which then leads to the further relativistic effect of strong light bending, Strong here implies a bending angle of up to a radian or more. Light bending then has the effect of making an intrinsically isotropic corona appear anisotropic to the outside observer. Primary power-law radiation from the corona is bent toward the disc (Fig. 1), enhancing the reflection spectrum and diminishing the observed primary continuum. Some of the observed variability can then be due to changes in source height (Miniutti & Fabian 2004) rather than the intrinsic luminosity. This can explain some of the puzzling variability seen in the AGN MCG–6-30-15 (Fabian et al 2003) and may have been observed in XTEJ1650-500 (Rossi et al 2005; Reis et al 2013).

Detailed modelling of the line shape in the best observed objects can reveal the extent of the corona (Wilkins & Fabian 2012) and its changes during luminosity variations (Wilkins et al (2014).

3. Reverberation

Soft X-ray reverberation has now been seen in about two dozen AGN (e.g. De Marco et al 2013; Emmanoulopoulos et al 2010; de Marco et al 2011; Kara et al 2013a; Alston et al 2013; Zoghbi & Fabian 2011). The reverberation timescales are of the order of the light cross time of a few gravitational radii (i.e.GM/c^2) implying that the corona is close to the black hole and the disc extends close in, so the black hole must spin rapidly. Iron-K reverberation is also now seen in about 9 AGN (Fig. 6. Kara et al 2014; Cackett et al 2013; Uttley et al 2014). Most of these results have been produced from the long continuous XMM light curves that are possible due to its 48 hr orbit. The $\sim$ 90 min low Earth orbits

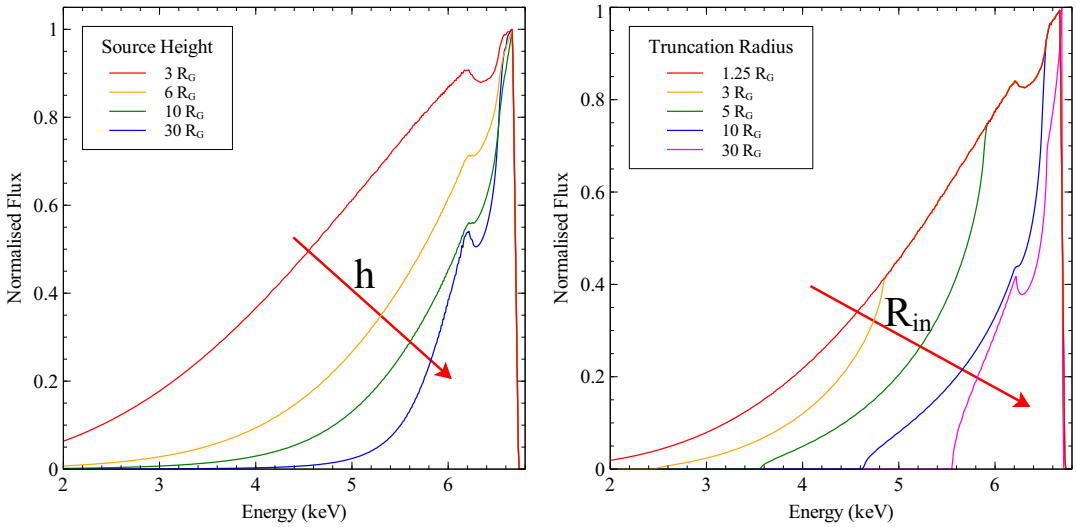

Fig. 5. Expected broad iron-K line profiles for a lampost corona. On the left the height of the corona is varied and on the right it is the inner edge of the disc. The black hole is rapidly spinning in all cases (Fabian et al 2014).

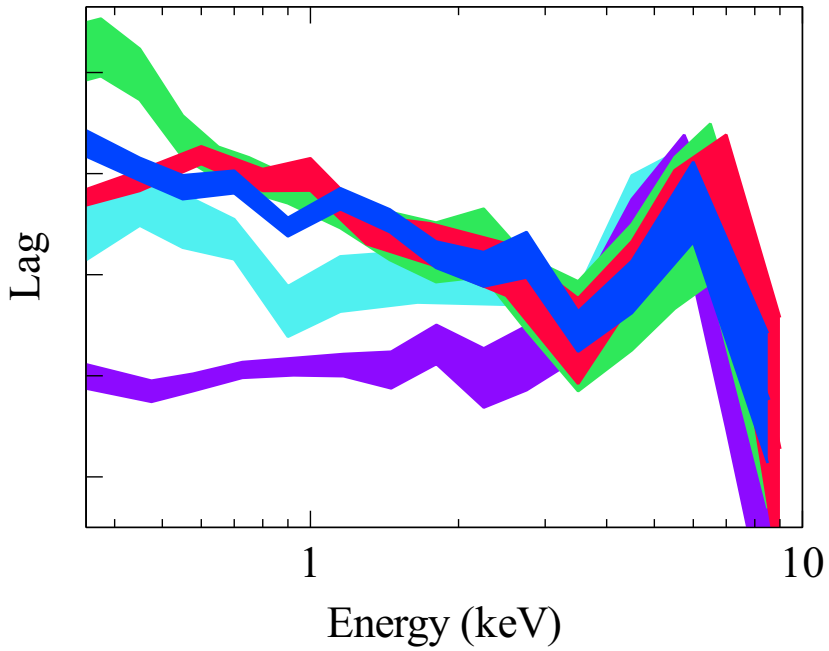

Fig. 6. The lag-energy spectra overplotted for five of the published sources with Fe K lags. The amplitude of the lag has been scaled so that the lag between 34 keV and 67 keV match for all sources. The sources shown are: 1H0707-495 (blue), IRAS 13224-3809 (red), Ark 564 (green), Mrk 335 (cyan) and PG 1244+026 (purple) (Kara et al 2014). While the shape of the Fe K lags are similar in all these sources, the lags associated with the soft excess vary.

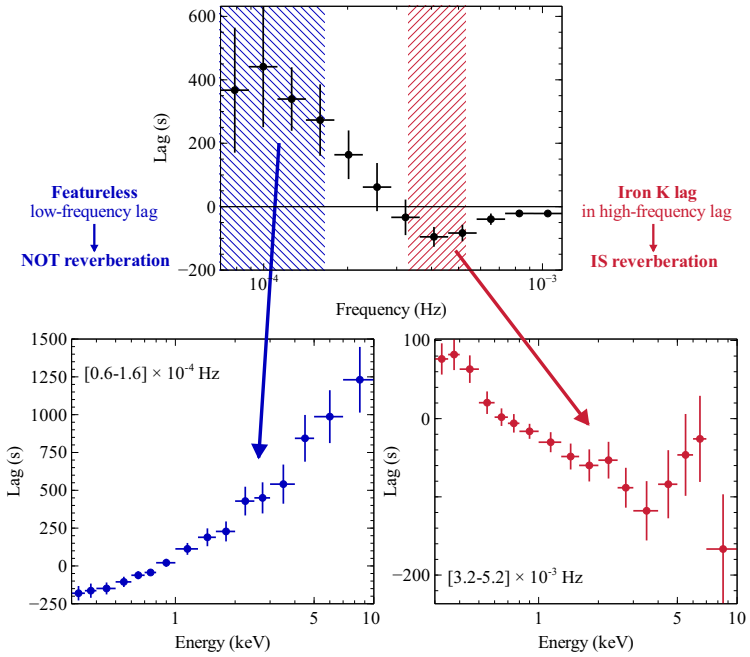

Fig. 7. Lag-frequency spectrum of Akn 564 is shown at the top, with the energy spectrum of the lags corresponding to the hatched2 frequency ranges shown nelow. To the left is the featureless low frequency lag spectrum. The high frequency lag spectrum shows a clear iron line confirming that it is due to reflection (Kara et al 2013b).

of Suzaku and NuSTAR produce chopped light curves which makes timing analyses challenging. Zoghbi et al (2013; 2014) have now overcome this problem with a maximum likelihood method.

Low frequency time lags were first seen in BHB such as Cyg X-1 by Miyamato & Kitamoto (1989) using GINGA data. They were observed at frequencies $f << 10^{-2} t_{\rm cross}^{-1}$, where $t_{cross} = GM/c^3$ the light crossing time of the black hole. At these frequencies propagation effects within the corona and changes in the corona, such as variations in spectral index, dominate. Low frequency lags were also seen in AGN (Vaughan et al. 2003; McHardy et al. 2004; Arévalo et al. 2006). The energy spectrum of the lags is a relatively featureless power-law or steady increase with energy (see also Walton et al 2013).

Reverberation dominates at *high* frequencies $f > 10^{-2} t_{\rm cross}^{-1}$. Observation of a broad iron line in the high frequency lags is a clear demonstration that they are due to reflection (Fig, 7; Kara et al 2013). This is a very important confirmation of the reflection scenario. Any alternative interpretation of the reflection features (e.g. complex distant absorption, Turner & Miller 2009; Miyakawa et al 2012) now requires an explanation for the high frequency, iron-K lags.

Modelling of the iron-K reverberation in NGC4151 (Fig. 8, Cackett et al 2014) yields good agreement with its mass of $5 \times 10^7\,{\rm M}_\odot$, measured by optical reverberation techniques.

4. Discussion

Relativistic disc lines are now seen in many luminous AGN and BHB. Absence of broad lines in unobscured AGN can be due to the corona being distant from the disc or outflowing at mildly relativistic velocities. Generally, however, the height of the corona is less than a few times the radius of the ISCO which means that the effects of strong gravity due to GR are important. These include gravitational redshifts, strong light bending and Shapiro time delays (implicit in the reverberation lags). X-ray spectral-timimg analyses of several of the most rapidly spinning black hole sources are giving us a window into the region within one gravitational radius of the event horizon, the very heart of the most luminous persistent sources of radiation in the Universe.

5. Acknowledgements

We thank the many colleagues who have contributed to the work reviewed here, including Phil Uttley, Jon Miller, Ed Cackett, Dan Wilkins, Chris Reynolds, Abdu Zoghbi, Dom Walton, Giorgio Matt, Fiona Harrison and the NuSTAR team.

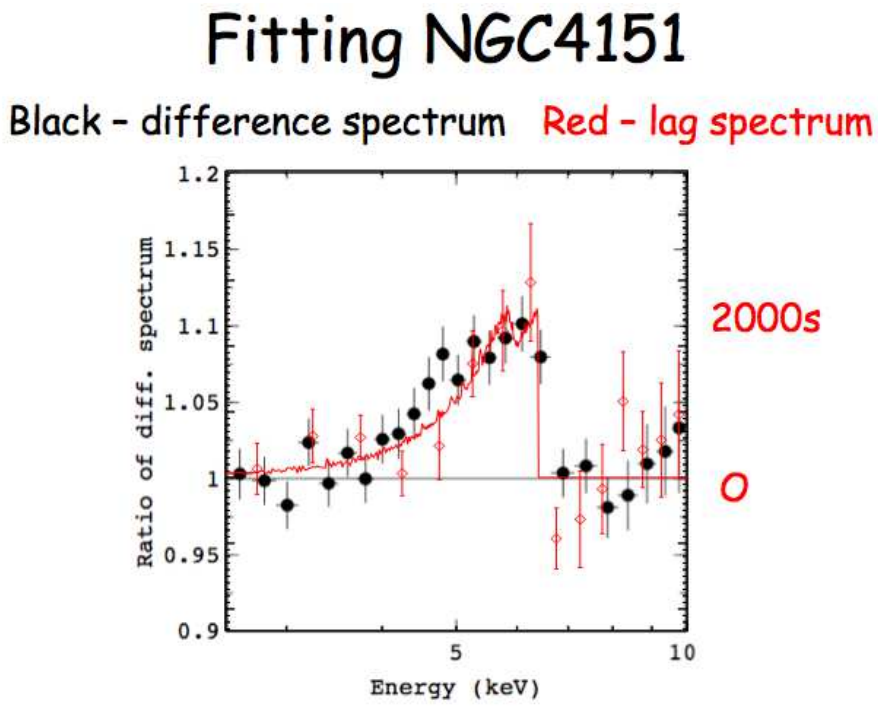

Fig. 8. The black points show the relativistic disc line spectrum in NGC4151 (left-hand axis, from a difference spectrum), whereas the red points show the lag-energy spectrum (right-hand axis). The agreement verifies that the black hole is rapidly spinning and has a mass close to 50 million $M_{\odot}$(Cackett et al 2014).

6. References

Alston, W. N., Vaughan, S., Uttley, P. 2013, MNRAS, 435, 1511
Cackett E et al 2013 ApJ, 720, L46
Cackett E. et al 2014 MNRAS 438 2980
De Marco B et al 2011 MNRAS, 417, L98
De Marco, B et al. 2013, MNRAS, 431, 2441
Emmanoulopoulos D. et al 2010, MNRAS, 404, 931
Fabian A.C. et al 1989 MNRAS, 238, 729
Fabian AC Vaughan S., 2003, MNRAS, 340, L282
Fabian AC Ross RR 2010 SpaceSciRev 157, 167
Fabian AC et al 2009 Nature, 459, 540
Fabian AC 2013 IAUS, 290, 3
Fabian AC et al 2014 MNRAS, 439, 2307
Garcia J et al 2014 ApJ, 782, 76
Kara, E., et al 2013a, MNRAS, 428, 2795
Kara, E., et al 2013b, MNRAS, 434, 1129
Kara E., et al 2014, MNRAS, 439, L26
Marinucci A., et al 2014, 440, 2347
Miller JM, 2007 ARAA 45 441
Miller J.M et al 2013 ApJ, 799, L2
Miller J.M et al 2013 ApJ, 775, L45
Miyakawa T., Ebisawa K., Inoue H., 2012, PASJ, 64, 140
Miyamoto S. Kitamoto S. 1989, Nature 342 773
Miniutti G., Fabian AC 2004 MNRAS, 349, 1435
Reis R.C., et al 2013, ApJ, 763, 48
Reynolds CR 2013 CQGRa, 30, 4004
Rossi S., et al 2005, MNRAS, 360, 763
Risaliti G., et al 2013, Nature, 494, 449
Ross R.R., Fabian A.C., 1993, MNRAS, 264, 839
Ross R.R., Fabian A.C., 2005, MNRAS, 358, 211
Tanaka Y et al 1995 Nature 375 659
Turner, T. J., Miller, L. 2009, A&ARev, 17, 47
TomsickJ., et al 2014, ApJ, 780, 78
Uttley P. et al 2014, A&ARev, in press
Walton DJ et al. 2013, ApJ, 777, L23
Wilkins D.R., Fabian A.C., 2012, MNRAS, 424, 1284
Wilkins D.R., Fabian A.C., 2013, MNRAS, 430, 247
Wilkins D.R., Fabian A.C., 2014, MNRAS, in press
Zoghbi A Fabian AC 2011 MNRAS, 418, 2642
Zoghbi, A., et al 2012, MNRAS, 422, 1
Zoghbi A., et al 2013, ApJ, 777, 25
Zoghbi A., et al 2014, ApJ, submitted